Bulletin of the Institute of Mathematics
Academia Sinica (New Series)
Vol. **2** (2007), No. 2, pp. 349-365

DETERMINISTIC AND STOCHASTIC SIMULATIONS OF ELECTRON TRANSPORT IN SEMICONDUCTORS

BY

MARTIN GALLER AND ARMANDO MAJORANA

Abstract

We present a new numerical scheme based on a shock capturing algorithm combined with a cell average method for solving the non-stationary Boltzmann-Poisson system describing the electron transport in semiconductor devices. The proposed computational technique is applied for investigating the carrier transport in a silicon MOSFET. Hydrodynamical and electrical quantities are shown and compared with data obtained by the Direct Simulation Monte Carlo (DSMC) method. The good agreement between the deterministic and the stochastic approaches validates the proposed numerical scheme, which may represent a useful tool for studying transport phenomena in semiconductors where the DSMC method does not give accurate results.

1. Introduction

Very large scale integration is the forthcoming design in semiconductor technology. This implies that in modern integrated electron devices the scale length of individual components becomes comparable with the distance between successive carrier interactions with the crystal, and the well-established drift-diffusion models describing the carrier transport lose their accuracy [1]. Consequently, to cope with high-field and sub-micron phenomena, Boltzmann transport equations (BTEs) must be applied [2]. Deterministic as well as stochastic procedures can be considered as solution approaches

Received November 29, 2004 and in revised form June 7, 2005.
AMS Subject Classification: 82D37, 82-08, 65M99.
Key words and phrases: Boltzmann equations, semiconductor, numerical schemes.

to these extremely sophisticated equations. So far, mainly stochastic methods have been applied to solve the BTEs [3]-[6]. Compared to stochastic methods, direct approaches provide noise-free resolution, high accuracy and easiness of arbitrary moment evaluations at low computational costs. The first finite difference approach to the Boltzmann transport equation was proposed by Fatemi and Odeh [7]. They developed an upwind finite difference approximation for the Boltzmann-Poisson system. Majorana and Pidatella [8] solved the Boltzmann-Poisson system by the help of a box method in the energy and angle variables and combined this approach with a classical discretization technique for advection equations based on upwinding in the spatial variable. Recently, Carrillo et al. [9], [10] succeeded in introducing a deterministic high-order finite difference Weighted Essentially Non Oscillatory (WENO) solver for the solution of the one-dimensional Boltzmann-Poisson system for semiconductor devices. Moreover, they extended their numerical technique to cope with spatially two-dimensional geometries [11]. In this paper, a cell average technique combined with a WENO scheme is proposed for solving the coupled Boltzmann-Poisson system. This new numerical scheme is based on the use of the cell average method for treating the dependence of the electron distribution function on the three-dimensional wave vector and a fifth-order WENO solver [10], [11] for dealing with the two-dimensional physical space. The resulting transport equations are applied for simulating the charge transport in a silicon MOSFET.

This paper is organized as follows. In Section 2, we introduce the basic equations and convert them in a suitable dimensionless form. In Section 3, we describe the new numerical scheme, and some results for a two-dimensional device are shown in Section 4. In the last section, we draw some conclusions and remarks.

2. The Boltzmann-Poisson System

The evolution of the electron distribution function $f(\mathrm{t}, \mathbf{x}, \mathbf{k})$ in semiconductors in dependence of time t, position $\mathbf{x}$ and electron wave vector $\mathbf{k}$ is governed by the Boltzmann transport equation (BTE) [12]

$$\frac{\partial f}{\partial \mathrm{t}} + \frac{1}{\hbar}\nabla_{\mathbf{k}}\,\varepsilon \cdot \nabla_{\mathbf{x}} f - \frac{q}{\hbar}\mathbf{E} \cdot \nabla_{\mathbf{k}} f = Q(f), \tag{1}$$

where $\hbar$ is the reduced Planck constant, and q denotes the positive elementary charge. The function $\varepsilon(\mathbf{k})$ is the energy of the considered crystal

conduction band measured from the band minimum; according to the Kane dispersion relation, ε is the positive root of

$$\varepsilon(1+\alpha\varepsilon) = \frac{\hbar^2 k^2}{2m^*}, \tag{2}$$

where α is the non-parabolicity factor and m^* the effective electron mass. The electric field $\mathbf{E}$ is related to the doping density N_D and the electron density n, which equals the zero-order moment of the electron distribution function f, by the Poisson equation

$$\nabla_{\mathbf{x}} \left[\epsilon_r(\mathbf{x})\, \nabla_{\mathbf{x}} V\right] = \frac{q}{\epsilon_0} \left[n(\mathrm{t},\mathbf{x}) - N_D(\mathbf{x})\right], \quad \mathbf{E} = -\nabla_{\mathbf{x}} V, \tag{3}$$

where ϵ_0 is the dielectric constant of the vacuum, $\epsilon_r(\mathbf{x})$ labels the relative dielectric function depending on the material and V the electrostatic potential. The collision operator $Q(f)$ takes into account acoustic deformation potential and optical intervalley scattering [13]. For low electron densities, it reads

$$Q(f)(\mathrm{t},\mathbf{x},\mathbf{k}) = \int_{\mathbb{R}^3} \left[S(\mathbf{k}',\mathbf{k}) f(\mathrm{t},\mathbf{x},\mathbf{k}') - S(\mathbf{k},\mathbf{k}') f(\mathrm{t},\mathbf{x},\mathbf{k})\right] d\mathbf{k}' \tag{4}$$

with the scattering kernel

$$\begin{aligned} S(\mathbf{k},\mathbf{k}') \;=\; & (n_q+1)\, K\, \delta(\varepsilon(\mathbf{k}') - \varepsilon(\mathbf{k}) + \hbar\omega_p) \\ & + n_q\, K\, \delta(\varepsilon(\mathbf{k}') - \varepsilon(\mathbf{k}) - \hbar\omega_p) + K_0\, \delta(\varepsilon(\mathbf{k}') - \varepsilon(\mathbf{k})) \end{aligned} \tag{5}$$

and K and K_0 being constant for silicon. The symbol δ indicates the usual Dirac distribution and ω_p is the constant phonon frequency. Moreover,

$$n_q = \left[\exp\left(\frac{\hbar\omega_p}{k_B T_L}\right) - 1\right]^{-1}$$

is the occupation number of phonons, k_B the Boltzmann constant and T_L the constant lattice temperature.

For the numerical treatment of the system (1), (3), it is convenient to introduce suitable dimensionless quantities and variables. We assume $T_L = 300\,K$. Typical values for length, time and voltage are $\ell_* = 10^{-6}\,m$, $t_* = 10^{-12}\,s$ and $V_* = 1\,\mathrm{Volt}$, respectively. Thus, we define the dimensionless variables

$$(x,y,z) = \frac{\mathbf{x}}{\ell_*}, \quad t = \frac{\mathrm{t}}{t_*}, \quad \Psi = \frac{V}{V_*}, \quad (E_x,E_y,E_z) = \frac{\mathbf{E}}{E_*}$$

with $E_* = 0.1\, V_*\, \ell_*^{-1}$ and

$$E_x = -c_v \frac{\partial \Psi}{\partial x}, \quad E_y = -c_v \frac{\partial \Psi}{\partial y}, \quad c_v = \frac{V_*}{\ell_* E_*}\,.$$

In correspondence to [8] and [10], we perform a coordinate transformation for $\mathbf{k}$ according to

$$\mathbf{k} = \frac{\sqrt{2m^* k_B T_L}}{\hbar} \sqrt{w(1+\alpha_K w)} \left(\mu, \sqrt{1-\mu^2}\cos\varphi, \sqrt{1-\mu^2}\sin\varphi\right), \qquad (6)$$

where the new independent variables are the dimensionless energy $w = \dfrac{\varepsilon}{k_B T_L}$, the cosine of the polar angle μ and the azimuth angle φ with $\alpha_K = k_B T_L \alpha$. The main advantage of the generalized spherical coordinates (6) is the easy treatment of the Dirac distribution in the kernel (5) of the collision term. In fact, this procedure enables us to transform the integral operator (4) with the not regular kernel S into an integral-difference operator, as shown in the following.

We are interested in studying two-dimensional problems in real space but, of course, in the whole three-dimensional $\mathbf{k}$-space. Therefore, it is useful to consider the new unknown function Φ related to the electron distribution function via

$$\Phi(t,x,y,w,\mu,\varphi) = s(w) f(\mathrm{t},\mathbf{x},\mathbf{k})\big|_{\mathrm{t}=t_* t,\ \mathbf{x}=\ell_*(x,y,z),\ \mathbf{k}=\frac{\sqrt{2m^* k_B T_L}}{\hbar}\sqrt{w(1+\alpha_K w)}\,\ldots},$$

where

$$s(w) = \sqrt{w(1+\alpha_K w)}(1+2\alpha_K w), \qquad (7)$$

is proportional to the Jacobian of the change of variables (6) and, apart from a dimensional constant factor, to the density of states. This allows us to write the free streaming operator of the dimensionless Boltzmann equation in a conservative form, which is appropriate for applying standard numerical schemes used for hyperbolic partial differential equations. Due to the symmetry of the problem and of the collision operator, we have

$$\Phi(t,x,y,w,\mu,2\pi-\varphi) = \Phi(t,x,y,w,\mu,\varphi)\,. \qquad (8)$$

Straightforward but cumbersome calculations end in the following transport equation for Φ:

$$\frac{\partial \Phi}{\partial t} + \frac{\partial}{\partial x}(g_1\Phi) + \frac{\partial}{\partial y}(g_2\Phi) + \frac{\partial}{\partial w}(g_3\Phi) + \frac{\partial}{\partial \mu}(g_4\Phi) + \frac{\partial}{\partial \varphi}(g_5\Phi) = C(\Phi)\,. \qquad (9)$$

The functions g_i $(i = 1, 2, \ldots, 5)$ in the advection terms depend on the independent variables w, μ, φ as well as on time and position via the electric field. They are given by

$$\begin{aligned}
g_1(\cdot) &= c_x \frac{\mu\sqrt{w(1+\alpha_K w)}}{1+2\alpha_K w},\\
g_2(\cdot) &= c_x \frac{\sqrt{1-\mu^2}\sqrt{w(1+\alpha_K w)}\cos\varphi}{1+2\alpha_K w},\\
g_3(\cdot) &= -2c_k \frac{\sqrt{w(1+\alpha_K w)}}{1+2\alpha_K w}\left[\mu\, E_x(t,x,y) + \sqrt{1-\mu^2}\cos\varphi\, E_y(t,x,y)\right],\\
g_4(\cdot) &= -c_k \frac{\sqrt{1-\mu^2}}{\sqrt{w(1+\alpha_K w)}}\left[\sqrt{1-\mu^2}\, E_x(t,x,y) - \mu\cos\varphi\, E_y(t,x,y)\right],\\
g_5(\cdot) &= c_k \frac{\sin\varphi}{\sqrt{w(1+\alpha_K w)}\sqrt{1-\mu^2}}\, E_y(t,x,y)
\end{aligned}$$

with

$$c_x = \frac{t_*}{\ell_*}\sqrt{\frac{2\,k_B T_L}{m^*}} \quad \text{and} \quad c_k = \frac{t_* q E_*}{\sqrt{2m^* k_B T_L}}\,.$$

The right hand side of (9) is the integral-difference operator

$$\begin{aligned}
&C(\Phi)(t,x,y,w,\mu,\varphi) = s(w)\left\{c_0\int_0^\pi d\varphi'\int_{-1}^1 d\mu'\,\Phi(t,x,y,w,\mu',\varphi')\right.\\
&\left.+\int_0^\pi d\varphi'\int_{-1}^1 d\mu'\,[c_+\Phi(t,x,y,w+\gamma,\mu',\varphi') + c_-\Phi(t,x,y,w-\gamma,\mu',\varphi')]\right\}\\
&-2\pi[c_0 s(w) + c_+ s(w-\gamma) + c_- s(w+\gamma)]\Phi(t,x,y,w,\mu,\varphi),
\end{aligned}$$

where

$$(c_0, c_+, c_-) = \frac{2m^*\,t_*}{\hbar^3}\sqrt{2\,m^*\,k_B T_L}\,(K_0, (n_q+1)K, n_q K)\,, \quad \gamma = \frac{\hbar\omega_p}{k_B T_L}$$

are dimensionless parameters. We remark that the δ distributions in the kernel S have been eliminated; this leads to the shifted arguments of Φ. The parameter γ represents the jump constant corresponding to the quantum of energy $\hbar\omega_p$. We have also taken into account (8) in the integration with respect to φ'.

In terms of the new variables the electron density becomes

$$n(t_*t, \ell_*x, \ell_*y) = \int_{\mathbb{R}^3} f(t_*t, \ell_*x, \ell_*y, \mathbf{k})\, d\mathbf{k} = \left(\frac{\sqrt{2\, m^* k_B T_L}}{\hbar}\right)^3 \rho(t, x, y),$$

where

$$\rho(t, x, y) = \int_0^{+\infty} dw \int_{-1}^{1} d\mu \int_0^{\pi} d\varphi\, \Phi(t, x, y, w, \mu, \varphi)\,. \tag{10}$$

Hence, the dimensionless Poisson equation writes

$$\frac{\partial}{\partial x}\left(\epsilon_r \frac{\partial \Psi}{\partial x}\right) + \frac{\partial}{\partial y}\left(\epsilon_r \frac{\partial \Psi}{\partial y}\right) = c_p\, [\rho(t, x, t) - \mathcal{N}_D(x, y)] \tag{11}$$

with

$$\mathcal{N}_D(x, y) = \left(\frac{\sqrt{2\, m^* k_B T_L}}{\hbar}\right)^{-3} N_D(\ell_* x, \ell_* y) \text{ and } c_p = \left(\frac{\sqrt{2\, m^* k_B T_L}}{\hbar}\right)^3 \frac{\ell_*^2 q}{\epsilon_0}\,.$$

Choosing the same values of the physical parameters as in [8], we obtain

$c_0 \approx 0.2653$	$c_x \approx 0.16857$	$c_p \approx 0.183 \times 10^7$
$c_+ \approx 0.507$	$c_k \approx 0.326067$	$c_v = 10.$
$c_- \approx 0.0443$		

3. Numerical Scheme

For obtaining approximate solutions to the coupled Boltzmann-Poisson system, we proceed as follows. The first step is to fix a maximum value w_{max} for the dimensionless energy. Of course, w_{max} must be related to the studied physical process, and we must check that $\Phi(t, x, y, w_{max}, \mu, \varphi)$ is negligible for all t, x, y, μ and φ.

Next, we choose three suitable integer numbers N_w, N_μ and N_φ and discretize the independent variables w, μ and φ via

$$\begin{aligned}
&w_{k+\frac{1}{2}} = k\,\Delta w, && k = 0, 1, \ldots, N_w, && \Delta w = w_{max}/N_w,\\
&\mu_{m+\frac{1}{2}} = -1 + m\,\Delta\mu, && m = 0, 1, \ldots, N_\mu, && \Delta\mu = 2/N_\mu,\\
&\varphi_{n+\frac{1}{2}} = n\,\Delta\varphi, && n = 0, 1, \ldots, N_\varphi, && \Delta\varphi = \pi/N_\varphi\,.
\end{aligned}$$

Here, we have taken into account that $\varphi \in [0, \pi]$. It is important to remark that N_w must be chosen in such way that $\sigma = \gamma/\Delta w \in \mathbb{N}$ in order to treat the shifted arguments in the collision operator correctly. We denote the generic cell in the (w, μ, φ) domain by

$$\mathcal{Z}_{kmn} = \left[w_{k-\frac{1}{2}}, w_{k+\frac{1}{2}}\right] \times \left[\mu_{m-\frac{1}{2}}, \mu_{m+\frac{1}{2}}\right] \times \left[\varphi_{n-\frac{1}{2}}, \varphi_{n+\frac{1}{2}}\right]$$

for $k = 1, 2, \ldots, N_w$, $m = 1, 2, \ldots, N_\mu$ and $n = 1, 2, \ldots, N_\varphi$. The center of the cell $\mathcal{Z}_{kmn}$ has the coordinates (w_k, μ_m, φ_n).

Let $p(w, \mu, \varphi)$ be an assigned nonnegative function. We assume that

$$\Phi(t, x, y, w, \mu, \varphi) = p(w, \mu, \varphi)\, G(t, x, y, w, \mu, \varphi), \tag{12}$$

where G represents the new unknown, and p has the role of a weight function. As our main assumption, we suggest that

$$G(t, x, y, w, \mu, \varphi) \approx G(t, x, y, w_k, \mu_m, \varphi_n) \tag{13}$$

for every t, x, y and (w, μ, φ) belonging to interior of the cell $\mathcal{Z}_{kmn}$. This implies that, if we integrate Eq. (9) over the cell $\mathcal{Z}_{kmn}$, the first term may be approximated as

$$\int_{\mathcal{Z}_{kmn}} \frac{\partial \Phi}{\partial t}\, dw d\mu d\varphi \approx \left[\int_{\mathcal{Z}_{kmn}} p(w, \mu, \varphi)\, dw d\mu d\varphi\right] \frac{\partial}{\partial t} G(t, x, y, w_k, \mu_m, \varphi_n)\,.$$

A further assumption is needed for considering the force terms, because, for instance,

$$\int_{\mathcal{Z}_{kmn}} \frac{\partial}{\partial w}(g_3 \Phi)\, dw d\mu d\varphi \tag{14}$$

$$= \int_{\mu_{m-\frac{1}{2}}}^{\mu_{m+\frac{1}{2}}} \int_{\varphi_{n-\frac{1}{2}}}^{\varphi_{n+\frac{1}{2}}} g_3(t, x, y, w, \mu, \varphi)\, p(w, \mu, \varphi)\, G(t, x, y, w, \mu, \varphi) d\mu d\varphi \Bigg|_{w_{k-\frac{1}{2}}}^{w_{k+\frac{1}{2}}}.$$

Here, it is reasonable to assume that the following approximation holds

$$G(t, x, y, w_{k\pm\frac{1}{2}}, \mu, \varphi) \approx G(t, x, y, w_{k\pm\frac{1}{2}}, \mu_m, \varphi_n) \tag{15}$$

for every (t, x, y) and $(\mu, \varphi) \in \left[\mu_{m-\frac{1}{2}}, \mu_{m+\frac{1}{2}}\right] \times \left[\varphi_{n-\frac{1}{2}}, \varphi_{n+\frac{1}{2}}\right]$. Consequently,

(14) can be approximated by

$$G(t,x,y,w,\mu_m,\varphi_n)\int_{\mu_{m-\frac{1}{2}}}^{\mu_{m+\frac{1}{2}}}\int_{\varphi_{n-\frac{1}{2}}}^{\varphi_{n+\frac{1}{2}}} g_3(t,x,y,w,\mu,\varphi)\,p(w,\mu,\varphi)\,d\mu d\varphi\Bigg|_{w_{k-\frac{1}{2}}}^{w_{k+\frac{1}{2}}}.$$

For simplifying the notation, we define

$$G_{k,m,n}(t,x,y) = G(t,x,y,w_k,\mu_m,\varphi_n) \quad (k,m,n\in\mathbb{N})$$

and

$$G_{q,r,s}(t,x,y) = G(t,x,y,w_q,\mu_r,\varphi_s),$$

where one of the indexes q,r,s is not an integer number. Now, it is our goal to derive a set of $N_w\times N_\mu\times N_\varphi$ equations for the $G_{k,m,n}$. The evolution equations for these unknowns are constructed as suggested by the method of weighted residuals [14]. The ansatz (12) is inserted into the dimensionless Boltzmann equation (9), and the result is integrated over each of the cells $\mathcal{Z}_{kmn}$. Introducing the approximations (13) and (15), we obtain the equations

$$\begin{aligned}
&A^{(0)}_{k,m,n}\frac{\partial}{\partial t}G_{k,m,n} + A^{(1)}_{k,m,n}\frac{\partial}{\partial x}G_{k,m,n} + A^{(2)}_{k,m,n}\frac{\partial}{\partial y}G_{k,m,n}\\
&+E_x(t,x,y)\left[A^{(3x)}_{k+\frac{1}{2},m,n}\,G_{k+\frac{1}{2},m,n} - A^{(3x)}_{k-\frac{1}{2},m,n}\,G_{k-\frac{1}{2},m,n}\right]\\
&+E_y(t,x,y)\left[A^{(3y)}_{k+\frac{1}{2},m,n}\,G_{k+\frac{1}{2},m,n} - A^{(3y)}_{k-\frac{1}{2},m,n}\,G_{k-\frac{1}{2},m,n}\right]\\
&+E_x(t,x,y)\left[A^{(4x)}_{k,m+\frac{1}{2},n}\,G_{k,m+\frac{1}{2},n} - A^{(4x)}_{k,m-\frac{1}{2},n}\,G_{k,m-\frac{1}{2},n}\right]\\
&+E_y(t,x,y)\left[A^{(4y)}_{k,m+\frac{1}{2},n}\,G_{k,m+\frac{1}{2},n} - A^{(4y)}_{k,m-\frac{1}{2},n}\,G_{k,m-\frac{1}{2},n}\right]\\
&+E_y(t,x,y)\left[A^{(5)}_{k,m,n+\frac{1}{2}}\,G_{k,m,n+\frac{1}{2}} - A^{(5)}_{k,m,n-\frac{1}{2}}\,G_{k,m,n-\frac{1}{2}}\right]\\
&=\sum_{\ell=1}^{N_\mu}\sum_{h=1}^{N_\varphi}\left[C^{(0)}_{k,\ell,h}\,G_{k,\ell,h} + C^{(+)}_{k,\ell,h}\,G_{k+\sigma,\ell,h} + C^{(-)}_{k,\ell,h}\,G_{k-\sigma,\ell,h}\right] - \nu_{k,m,n}\,G_{k,m,n}
\end{aligned} \tag{16}$$

for each (k,m,n) so that $1\le k\le N_w$, $1\le m\le N_\mu$ and $1\le n\le N_\varphi$. The

coefficients

$$
\begin{aligned}
A^{(0)}_{k,m,n} &= \int_{\mathcal{Z}_{kmn}} p(w,\mu,\varphi)\, dwd\mu d\varphi \\
A^{(1)}_{k,m,n} &= \int_{\mathcal{Z}_{kmn}} g_1(w,\mu)\, p(w,\mu,\varphi)\, dwd\mu d\varphi \\
A^{(2)}_{k,m,n} &= \int_{\mathcal{Z}_{kmn}} g_2(w,\mu,\varphi)\, p(w,\mu,\varphi)\, dwd\mu d\varphi \\
A^{(3x)}_{k\pm\frac{1}{2},m,n} &= \int_{\mu_{m-\frac{1}{2}}}^{\mu_{m+\frac{1}{2}}} \int_{\varphi_{n-\frac{1}{2}}}^{\varphi_{n+\frac{1}{2}}} g_{3x}(w_{k\pm\frac{1}{2}},\mu,\varphi)\, p(w_{k\pm\frac{1}{2}},\mu,\varphi)\, d\mu d\varphi \\
A^{(3y)}_{k\pm\frac{1}{2},m,n} &= \int_{\mu_{m-\frac{1}{2}}}^{\mu_{m+\frac{1}{2}}} \int_{\varphi_{n-\frac{1}{2}}}^{\varphi_{n+\frac{1}{2}}} g_{3y}(w_{k\pm\frac{1}{2}},\mu,\varphi)\, p(w_{k\pm\frac{1}{2}},\mu,\varphi)\, d\mu d\varphi \\
A^{(4x)}_{k,m\pm\frac{1}{2},n} &= \int_{w_{k-\frac{1}{2}}}^{w_{k+\frac{1}{2}}} \int_{\varphi_{n-\frac{1}{2}}}^{\varphi_{n+\frac{1}{2}}} g_{4x}(w,\mu_{m\pm\frac{1}{2}},\varphi)\, p(w,\mu_{m\pm\frac{1}{2}},\varphi)\, dwd\varphi \\
A^{(4y)}_{k,m\pm\frac{1}{2},n} &= \int_{w_{k-\frac{1}{2}}}^{w_{k+\frac{1}{2}}} \int_{\varphi_{n-\frac{1}{2}}}^{\varphi_{n+\frac{1}{2}}} g_{4y}(w,\mu_{m\pm\frac{1}{2}},\varphi)\, p(w,\mu_{m\pm\frac{1}{2}},\varphi)\, dwd\varphi \\
A^{(5)}_{k,m,n\pm\frac{1}{2}} &= \int_{w_{k-\frac{1}{2}}}^{w_{k+\frac{1}{2}}} \int_{\mu_{m-\frac{1}{2}}}^{\mu_{m+\frac{1}{2}}} g_{5y}(w,\mu,\varphi_{n\pm\frac{1}{2}})\, p(w,\mu,\varphi_{n\pm\frac{1}{2}})\, dwd\mu \\
C^{(0)}_{k,m,n} &= c_0 \Delta\mu\Delta\varphi \int_{\mathcal{Z}_{kmn}} s(w)\, p(w,\mu',\varphi')\, dwd\mu' d\varphi' \\
C^{(+)}_{k,m,n} &= c_+ \Delta\mu\Delta\varphi \int_{\mathcal{Z}_{kmn}} s(w)\, p(w+\gamma,\mu',\varphi')\, dwd\mu' d\varphi' \\
C^{(-)}_{k,m,n} &= c_- \Delta\mu\Delta\varphi \int_{\mathcal{Z}_{kmn}} s(w)\, p(w-\gamma,\mu',\varphi')\, dwd\mu' d\varphi' \\
\nu_{k,m,n} &= 2\pi \int_{\mathcal{Z}_{kmn}} [c_0 s(w) + c_+ s(w-\gamma) + c_- s(w+\gamma)]\, p(w,\mu,\varphi)\, dwd\mu d\varphi
\end{aligned}
$$

depend only on the grid in the (w,μ,φ) domain and can be evaluated when the weight function p is chosen. The new functions $g_{3x}(w,\mu,\varphi)$ and $g_{3y}(w,\mu,\varphi)$ are the coefficients of $E_x(t,x,y)$ and $E_y(t,x,y)$ in g_3, respectively, i.e.,

$$g_3(t,x,y,w,\mu,\varphi) = g_{3x}(w,\mu,\varphi)\, E_x(t,x,y) + g_{3y}(w,\mu,\varphi) E_y(t,x,y)\,.$$

The functions g_{4x}, g_{4y} and g_{5y} are defined in the same way. On the right hand side of (16), we set $G_{k\pm\sigma,\ell,h} = 0$ when $k \pm \sigma$ does not belong to the interval $[1, N_w]$. We observe that the system (16) is still not closed because of the

appearing of the functions $G_{q,r,s}$. Hence, we need to choose an approximation of these functions in terms of $G_{k,m,n}$ $(k,m,n \in \mathbb{N})$. A simple formula for solving this problem is given by the Min-Mod slope limiter [15]. Let us consider the expression

$$E_x(t,x,y)\, A^{(3x)}_{k+\frac{1}{2},m,n}\, G_{k+\frac{1}{2},m,n}\,,$$

which is the first $G_{q,r,s}$ term in Eqs. (16). To avoid cumbersome expressions, we denote $E_x(t,x,y)\, A^{(3x)}_{k+\frac{1}{2},m,n}$ by a. For fixed (t,x,y) and (n,m), the value of a is determined, and a simple Taylor expansion results in

$$G_{k+\frac{1}{2},m,n} \approx \begin{cases} G_{k,m,n} + \dfrac{\Delta w}{2}\, G'_{k,m,n} & \text{if } a > 0 \\ G_{k+1,m,n} - \dfrac{\Delta w}{2}\, G'_{k+1,m,n} & \text{if } a < 0 \end{cases}, \tag{17}$$

where, only in this section, primes denote partial derivatives with respect to w. Of course, the case of vanishing a need not be considered. Equation (17) allows us to replace the function $G_{k+\frac{1}{2},m,n}$ with an approximation containing $G_{k,m,n}$ or $G_{k+1,m,n}$, but also one derivative. Taking into account the hyperbolic character of Eqs. (16), we define for $a > 0$

$$d_- = \frac{G_{k,m,n} - G_{k-1,m,n}}{\Delta w}, \quad d_+ = \frac{G_{k+1,m,n} - G_{k,m,n}}{\Delta w}$$

and approximate the sought derivative according to

$$G'_{k,m,n} \approx \begin{cases} \min\{|d_-|, |d_+|\}\, \mathrm{sgn}(d_-) & \text{if } d_- d_+ > 0 \\ 0 & \text{otherwise} \end{cases}.$$

For $a < 0$, a similar formula holds. All the other functions $G_{q,r,s}$ in Eqs. (16) are approximated analogously, except for the term including $A^{(4y)}$, where a little rearrangement is necessary. In fact, the correct use of the Min-Mod slope limiter requires a possessing a constant sign in the small neighborhood where the approximation is performed. Thus, we write

$$\begin{aligned} g_{4y}(w,\mu,\varphi) &= c_k \frac{\sqrt{1-\mu^2}}{\sqrt{w(1+\alpha_K w)}} \mu \cos\varphi \\ &= c_k \frac{\sqrt{1-\mu^2}}{\sqrt{w(1+\alpha_K w)}} (\mu - 1) \cos\varphi + c_k \frac{\sqrt{1-\mu^2}}{\sqrt{w(1+\alpha_K w)}} \cos\varphi \end{aligned}$$

and consider $A^{(4y)}$ as a sum of two coefficients of $G_{k,m\pm\frac{1}{2},n}$ having a definite

sign. In this way, we have a (large) system of partial differential equations with the independent variables t, x and y. This approach, consisting in the approximation of the Boltzmann equation by means of a system of partial differential equations, follows the main idea of Ringhofer [17], where the transport equation for semiconductors was studied in the framework of Hilbert spaces. The treatment of the new set of equations, obtained from (16), requires methods suitable for hyperbolic equations in conservative form. These schemes must be accurate also in presence of strong gradients. The WENO scheme has given excellent results when solving Eqs. (1), (3), hence, we continue to use this method for treating the partial derivatives with respect to x and y. This technique gives a final set of ordinary differential equations in time, which are integrated using TVD Runge-Kutta formulas [16]. Some very preliminary results were shown in [18], where we assumed $p = 1$ and applied this numerical technique for investigating carrier transport in bulk silicon, in a $n^+ - n - n^+$ diode and in a silicon MESFET. The results were compared to those of a full WENO solver [10], [11] exhibiting perfect agreement. This is due to the regularity of the distribution function with respect to the coordinates w, μ and φ. So, also the proposed scheme, which is of order less then the full WENO solver, gives accurate solutions.

4. Numerical Results

In this paper, we show the results of a numerical solution of the Boltzmann-Poisson system by assuming the weight p equal to the function $s(w)$ given by (7). The new numerical scheme is applied to a well-known two-dimensional silicon device, called MOSFET (see Figure 1). The holes are completely neglected in this simulation.

The doping density N_D is chosen equal to $3 \times 10^{17} \mathrm{cm}^{-3}$ in the n^+ regions and null in the other part of the device. Hence, the bulk substrate is treated as intrinsic silicon. The source and drain contacts are modeled as ohmic contacts, which allow the electrons to enter and exit the device. Perfectly reflecting boundary conditions are imposed at the $\mathrm{Si/SiO_2}$ interface and at all of the non-contact surfaces of the MOSFET.

The electrostatic potential is assigned to $V_S = 0 \times V_*$ at source, $V_G = 0.4 \times V_*$ at gate and $V_D = 1 \times V_*$ at drain. Moreover, we assume vanishing electric field in the direction normal to the surface at the bottom, right and left sides, and at the top where there are no contacts. The relative dielectric

function ϵ_r holds the value 3.9 in the SiO_2 region and 11.7 in the other part of the device.

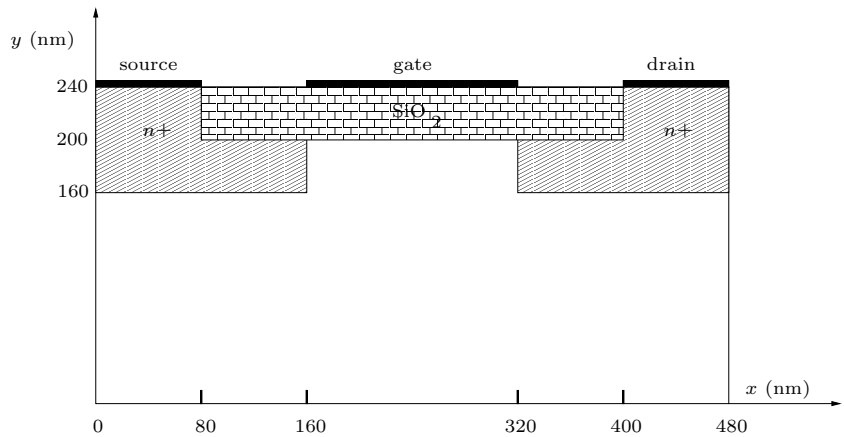

Figure 1. Schematic illustration of a 2D-MOSFET.

Since we study a time dependent problem, initial conditions must be fixed. We choose the distribution function $f(0, \mathbf{x}, \mathbf{k})$ to be given by a Maxwellian of zero bulk velocity at lattice temperature T_L and the initial density equal to the donor density. It is easy to derive the initial data for the coefficients $G_{k,m,n}$. The number of grid points in the (x, y) domain is set to 49×25. Moreover, we choose $N_w = 33$, $N_\mu = 8$, $N_\varphi = 8$ and $\sigma = 3$. Some figures show the results of the numerical simulation at the final time (5 ps). In Figure 2, we exhibit two main moments of the distribution function,

$$n(\mathrm{t}, \mathbf{x}) = \int_{\mathbb{R}^3} f(\mathrm{t}, \mathbf{x}, \mathbf{k})\, d\mathbf{k}, \quad \mathcal{E}(\mathrm{t}, \mathbf{x}) = \frac{1}{n(\mathrm{t}, \mathbf{k})} \int_{\mathbb{R}^3} f(\mathrm{t}, \mathbf{x}, \mathbf{k})\, \varepsilon(\mathbf{k})\, d\mathbf{k}, \quad (18)$$

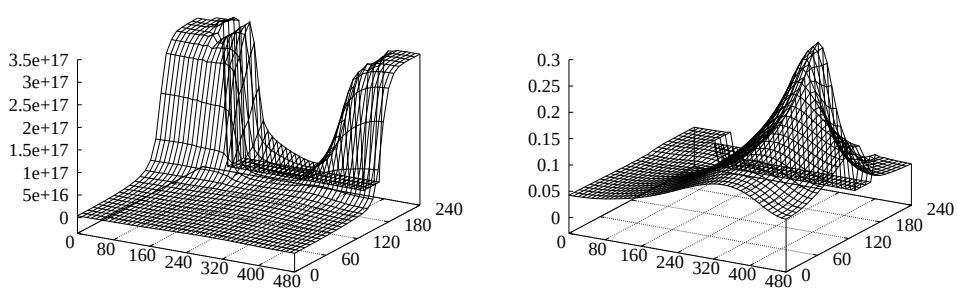

Figure 2. Electron density (in cm^{-3}) and energy (in eV).

namely the electron density and the hydrodynamical energy. The integrals (18) are evaluated using the simple midpoint rule.

Figure 3 shows the velocity field and the current lines versus position as well as the electrostatic potential. We also compare some hydrodynamical quantities in the stationary regime with the corresponding data obtained by the DSMC method. The graphics of the electrostatic potential and the electric field coincide in both simulations. When density, velocity or energy are considered, we observe a few differences in some points of the device.

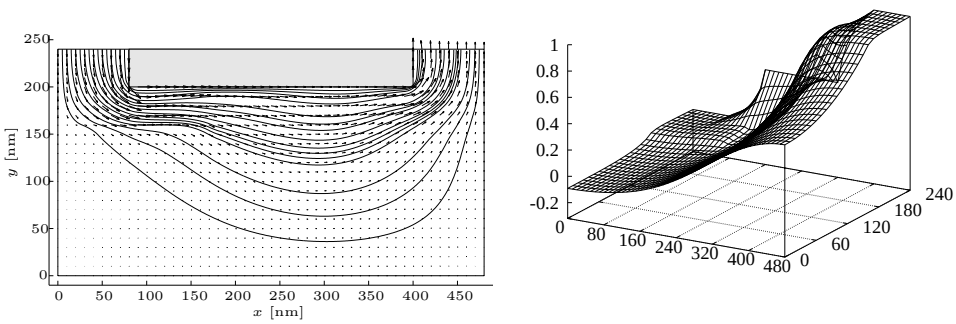

Figure 3. Velocity field and electrical potential (in Volt).

In order to show these differences by means of meaningful and clear figures, we plot some cuts of these quantities for $y = 40, 120, 160$ and 200 nm.

Figures 4, 5, 6 and 7 show the electron density, the two components of the hydrodynamical velocity and the energy, respectively. We note an excellent agreement in some parts and evident differences in other ones.

In our opinion, most of the differences are due to a poor accuracy of DSMC results because they are located in regions where the distribution function is smooth enough for regarding the numerical solution of the Boltzmann-Poisson system as being accurate. Since in some of these zones the charge density is low, it is obvious that Monte Carlo simulations cannot furnish good results. The other possible reason for these differences arises from the fact that it is difficult to impose exactly corresponding boundary conditions for the two models (BTE and DSMC).

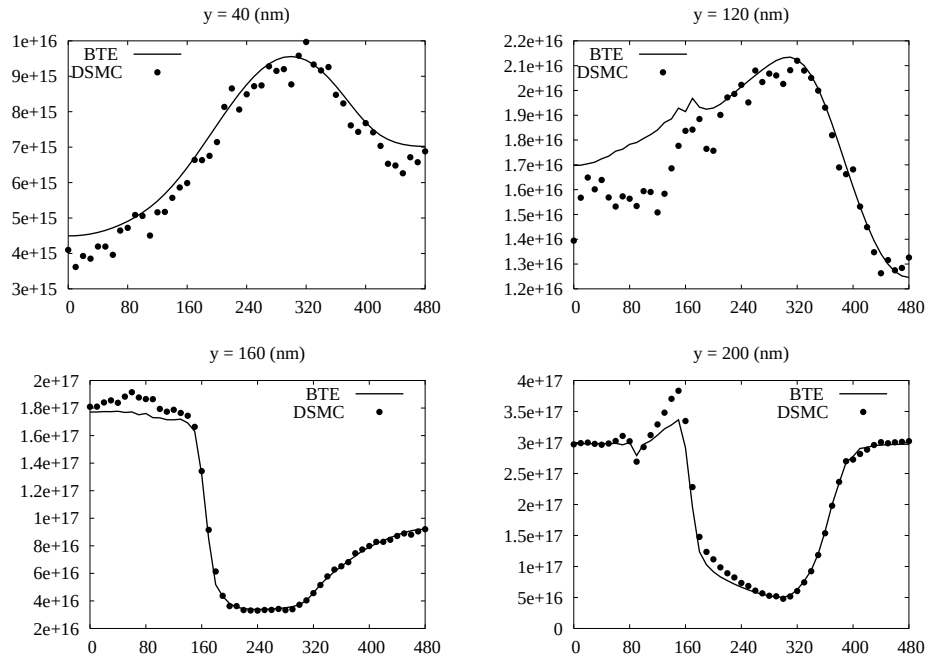

Figure 4. BTE and DSMC results: density of charge (in cm^{-3}).

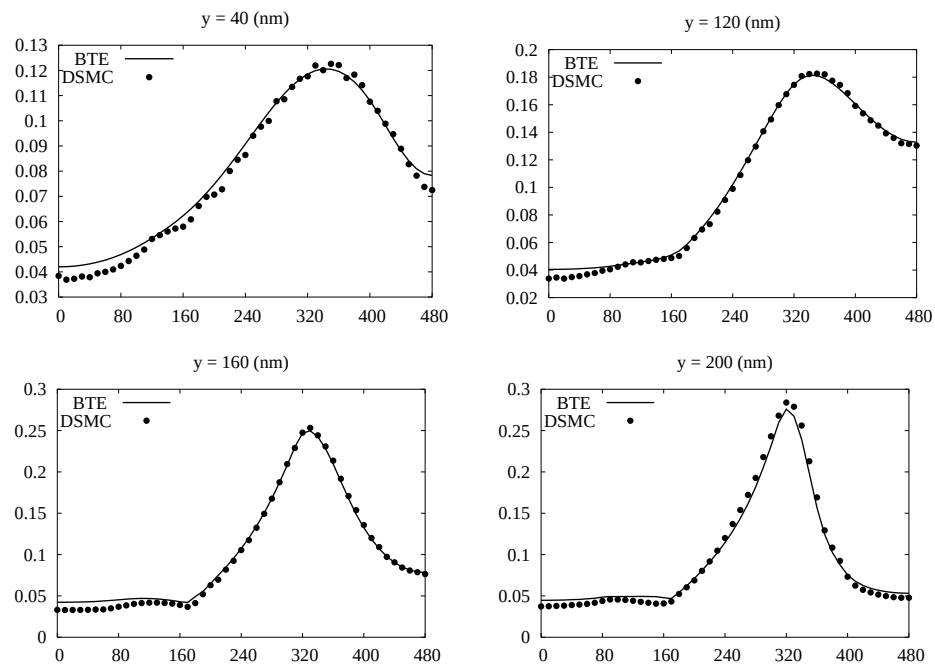

Figure 5. BTE and DSMC results: energy (in eV).

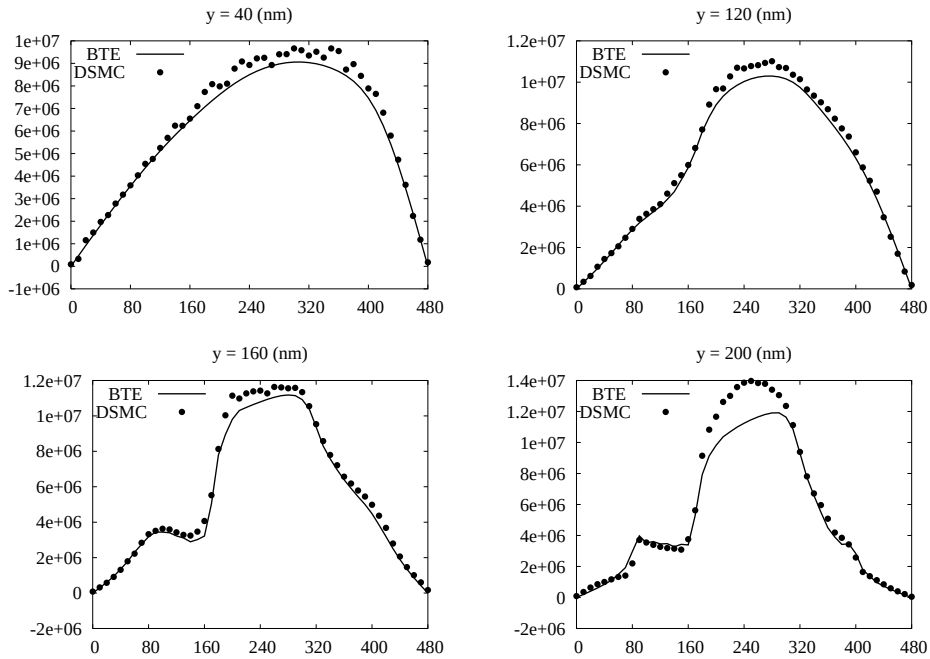

Figure 6. BTE and DSMC results: x-component of the velocity (in cm s^{-1}).

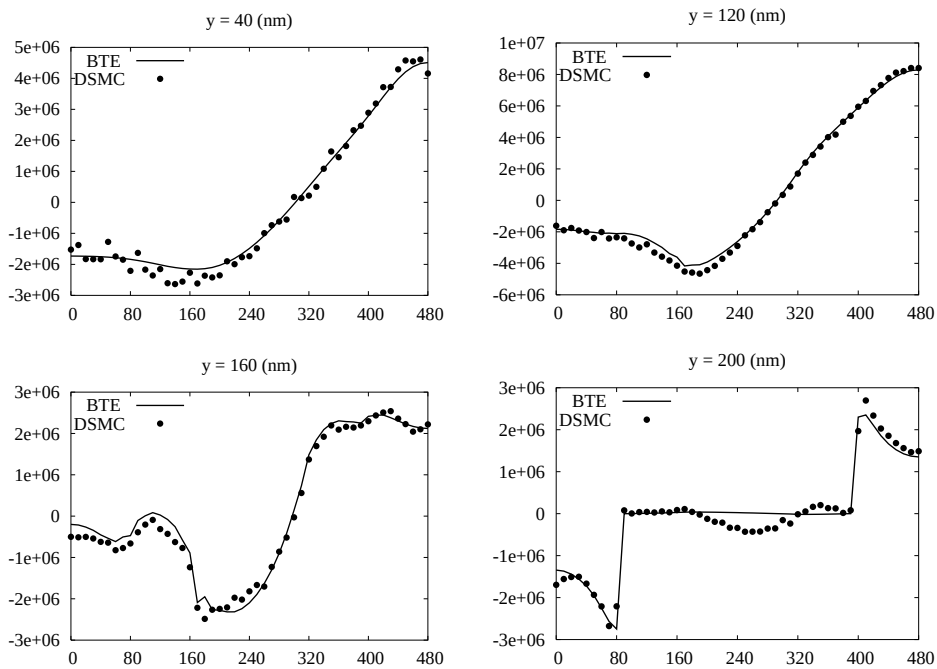

Figure 7. BTE and DSMC results: y-component of the velocity (in cm s^{-1}).

5. Conclusion

Numerical solutions of the system (1), (3) allow us to obtain useful information and data on transport phenomena in semiconductors. In addition, this approach represents an important tool for comparing hydrodynamical and electrical variables with the corresponding quantities obtained by solving other models, as DSMC, drift diffusion or energy transport equations.

The presented new numerical scheme seems to be accurate though its order is less than that of the full WENO solver. Moreover, it is less CPU time consuming which is a clear advantage in 2D simulations. In the test shown in this paper, we found that the use of the simplest first order Runge-Kutta (the explicit Euler) formula is sufficient for solving the system of the ordinary differential equations. A final remark concerns the application of the weight function $p = s(w)$. The main reason for this choice is the presence of the singularity of the coefficients g_4 and g_5 for vanishing dimensionless energy w. When the new unknown G is introduced, these singularities disappear. Moreover, this function is, apart from a constant factor, the old distribution function f, which is regular near $\mathbf{k} = 0$, where the energy $\varepsilon(\mathbf{k}) = 0$.

Acknowledgments

This work was supported by the Fond zur Förderung der wissenschaftlichen Forschung, Vienna, under contract number P14669-TPH, by the European community programme IHP, contract number HPRN-CT-2002-00282 on behalf of the CNR and by M.U.R.S.T. Cofin 2002 *Mathematical problem of Kinetic Theories*.

References

1. P. A. Markowich, C. Ringhofer and C. Schmeiser, *Semiconductor Equations*, Springer-Verlag, New York, 1990.

2. D. K. Ferry, *Semiconductors*, Maxwell MacMillian, New York, 1991.

3. C. Jacoboni and P. Lugli, *The Monte Carlo Method for Semiconductor Device Simulation*, Spring Verlag, Wien-New York, 1989.

4. K. Tomizawa, *Numerical Simulation of Sub Micron Semiconductor Devices*, Artech House, Boston, 1993.

5. C. Jacoboni and L. Reggiani, The Monte Carlo method for the solution of charge transport in semiconductor with application to covalent materials, *Rev. Modern Phys.* **55**(1983), 645-705.

6. M. V. Fischetti, Monte Carlo simulation of transport in technologically significant semiconductors of the diamond and Zinc-BlendeStructures - Part I: homogeneous transport, *IEEE Trans. Elec. Dev.* **38**(1991), 634–649.

7. E. Fatemi and F. Odeh, Upwind finite difference solution of Boltzmann equation applied to electron transport in semiconductor devices, *J. Comput. Phys.*, **108**(1993), 209-217.

8. A. Majorana and R. M. Pidatella, A finite difference scheme solving the Boltzmann-Poisson system for semiconductor devices, *J. Comput. Phys.*, **174**(2001), 649-668.

9. J. A. Carrillo, I. M. Gamba, A. Majorana and C.-W. Shu, A WENO-solver for 1D non-stationary Boltzmann-Poisson system for semiconductor devices, *J. Comp. Electr.*, **1**(2002), 365-375.

10. J. A. Carrillo, I. M. Gamba, A. Majorana and C.-W. Shu, A WENO-solver for the transients of Boltzmann-Poisson system for semiconductor devices. Performance and comparisons with Monte Carlo methods, *J. Comp. Phys.*, **184**(2003), 498-525.

11. J. A. Carrillo, I. M. Gamba, A. Majorana and C.-W. Shu, A direct solver for 2D non-stationary Boltzmann-Poisson systems for semiconductor devices: a MESFET simulation by WENO-Boltzmann schemes, *J. Comput. Electr.* **2**(2003), 375-380.

12. M. Lundstrom, *Fundamentals of Carrier Transport*, Cambridge University Press, Cambridge, 2000.

13. J. M. Ziman, *Electrons and Phonons. The Theory of Transport Phenomena in Solids*, Oxford University Press, Oxford, 2000.

14. L. Lapidus and G. F. Pinder, *Numerical Solution of Partial Differential Equations in Science and Engineering*, Wiley, New York, 1982.

15. R. J. LeVeque, *Numerical Methods for Conservation Laws*, Birkhäuser, Basel, 1992.

16. C.-W. Shu and S. Osher, Efficient implementation of essentially non-oscillatory shock capturing schemes, *J. Comp. Phys.*, **77**(1988), 439-471.

17. C. Ringhofer, Space-time discretization of series expansion methods for the Boltzmann Transport equation, *SIAM J. Numer. Anal.*, **38**(2000), 442-465.

18. M. Galler, A. Majorana and F. Schürrer, A Multigroup-WENO Solver for the Non-Stationary Boltzmann-Poisson System for Semiconductor Devices, In Proceedings of SCEE 2004, Capo d'Orlando, Italy, Sept. 5-9, 2004.

Institute of Theoretical and Computational Physics, Graz University of Technology, Graz, Austria.
E-mail: E-mail: galler@itp.tu-graz.ac.at

Dipartimento di Matematica e Informatica, Università di Catania, Catania, Italy.
E-mail: E-mail: majorana@dmi.unict.it